

Supplementary Information for “Long-range magnetic order in real icosahedral quasicrystals”

Ryuji Tamura^{1*}, Asuka Ishikawa², Shintaro Suzuki¹, Akihiro Kotajima¹, Yujiro Tanaka¹, Takehito Seki³, Naoya Shibata³, Tsunetomo Yamada⁴, Takenori Fujii⁵, Chin-Wei Wang⁶, Maxim Avdeev^{7,8} and Taku J. Sato^{9*}

¹Department of Materials Science and Technology, Tokyo University of Science, Katsushika, Tokyo 125-8585, Japan,

²Research Institute for Science and Technology, Tokyo University of Science, Katsushika, Tokyo 125-8585, Japan,

³Institute of Engineering Innovation, School of Engineering, The University of Tokyo, Bunkyo, Tokyo 113-8656, Japan,

⁴Department of Applied Physics, Tokyo University of Science, Katsushika, Tokyo 125-8585, Japan,

⁵Cryogenic Research Center, The University of Tokyo, Bunkyo, Tokyo 113-0032, Japan,

⁶National Synchrotron Radiation Research Center, Hsinchu 30076, Taiwan,

⁷Australian Nuclear Science and Technology Organisation, New Illawarra Road, Lucas Heights, NSW 2234, Australia,

⁸School of Chemistry, The University of Sydney, Sydney, NSW 2006, Australia,

⁹Institute of Multidisciplinary Research for Advanced Materials, Tohoku University, 2-1-1 Katahira, Aoba, Sendai 980-8577, Japan

1. Magnetization measurements on $\text{Au}_{65}\text{Ga}_{20}R_{15}$ ($R = \text{Gd}, \text{Tb}$) *i* QCs

Figure S1 shows the inverse magnetic susceptibility $1/\chi = H/M$ as a function of the temperature from 2 to 300 K for $\text{Au}_{65}\text{Ga}_{20}R_{15}$ ($R = \text{Gd}, \text{Tb}$) *i* QCs. As can be seen from the linearity in both the $1/\chi - T$ curves, the magnetic susceptibility well obeys the Curie–Weiss law $\chi = N_A \mu_{\text{eff}}^2 / (3k_B(T - \theta))$ for both *i* QCs, where N_A denotes the Avogadro number, k_B the Boltzmann constant, and θ the Weiss temperature. The effective magnetic moments μ_{eff} obtained from the fitting are $7.90\mu_B$ for *i* $\text{Au}_{65}\text{Ga}_{20}\text{Gd}_{15}$ and $9.64\mu_B$ for *i* $\text{Au}_{65}\text{Ga}_{20}\text{Tb}_{15}$, which are in good agreement with the theoretical values of R^{3+} ($R = \text{Gd}, \text{Tb}$) free ions, $7.94\mu_B$ and $9.72\mu_B$, respectively. The θ values are 27.9 K for *i* $\text{Au}_{65}\text{Ga}_{20}\text{Gd}_{15}$ and 12.9 K for *i* $\text{Au}_{65}\text{Ga}_{20}\text{Tb}_{15}$, which means that the inter-spin interactions are predominantly *ferromagnetic* for these *i* QCs, unlike all the other *i* QCs reported to date.

Figure S2 shows magnetic field dependences of the magnetization M measured at $T = 2$ K, for (a) the $\text{Au}_{65}\text{Ga}_{20}\text{Gd}_{15}$ and (b) $\text{Au}_{65}\text{Ga}_{20}\text{Tb}_{15}$ *i* QCs. For *i* $\text{Au}_{65}\text{Ga}_{20}\text{Gd}_{15}$, M quickly saturates to $\sim 7\mu_B/\text{Gd}^{3+}$, nearly the full moment of a free Gd^{3+} ion ($7\mu_B/\text{Gd}^{3+}$), at a low field of 100 Oe. On the other hand, for *i* $\text{Au}_{65}\text{Ga}_{20}\text{Tb}_{15}$, the M magnitude is suppressed to $\sim 6\mu_B/\text{Tb}^{3+}$ at 7 T, about two-thirds of the full moment of the Tb^{3+} ion ($9\mu_B/\text{Tb}^{3+}$). Here, the quick magnetic saturation in *i* $\text{Au}_{65}\text{Ga}_{20}\text{Gd}_{15}$ is a characteristic

feature of ferromagnets with weak magnetic anisotropy. On the other hand, the M suppression in i Au₆₅Ga₂₀Tb₁₅ is due to a strong uniaxial anisotropy of Tb³⁺ spins (as described in the text).

2. Powder-neutron-diffraction experiments on i Au₆₅Ga₂₀Tb₁₅ and 1/1

Au₆₅Ga₂₀Tb₁₅.

Figure S3(a) shows the powder-neutron-diffraction patterns of i Au₆₅Ga₂₀Tb₁₅ measured at various temperatures in a range $3.5 < T < 40$ K, across the anomaly temperature of $T_C = 16$ K observed in the bulk magnetic measurements. Below $T_C = 16$ K, new Bragg peaks, as well as enhancement of the reflection intensity at nuclear Bragg positions, are clearly observed in a low- 2θ region. A closer inspection of their temperature dependences reveals that there exist two sets of peaks with different transition temperatures. This is exemplified in Fig. S3(b), which shows a magnified diffraction pattern for $20^\circ < 2\theta < 33^\circ$. The lower-angle peak at $2\theta = 21.4^\circ$ disappears at 14 K, whereas the higher-angle peak at $2\theta = 31.8^\circ$ still retains some intensity at 14 K, indicating that the phase contributing to the lower-angle magnetic reflection has a slightly lower transition temperature below 14 K. Since the present i QC sample contains a small amount of 1/1 AC phase as indicated by the powder x-ray diffraction

(Fig. 2), we speculate that the secondary set of magnetic reflections with the lower transition temperature stems from the magnetic order of this contaminating 1/1 AC phase.

In order to test this hypothesis, we prepared pure phase of 1/1 Au-Ga-Tb AC with the same nominal composition as that of the *i* QC phase and performed neutron powder diffraction experiments on it. The single AC phase was obtained by annealing the sample, prepared by arc melting, at 923 K for 50 h. The neutron powder diffraction patterns of the 1/1 Au-Ga-Tb AC at the base temperature (3.5 K) and the paramagnetic temperature (20 K) are shown in Fig. S4. The diffraction pattern at 3.5 K clearly shows appearance of magnetic Bragg reflections, which can be indexed using the antiferromagnetic modulation vector $\mathbf{q} = (1, 1, 1)$, similar to the case of the previously investigated 1/1 Au-Al-Tb AC¹. Note that this magnetic modulation vector breaks bcc translational symmetry of the chemical lattice of the 1/1 AC, and therefore, the magnetic peaks appear in addition to the nuclear reflection positions.

By comparing the diffraction pattern of the 1/1 AC to that of the present *i* QC sample, one finds that the peaks appearing at $2\theta = 21.4^\circ, 34.8^\circ, 40.0^\circ, 42.4^\circ$ and 44.7° are commonly observed in both the samples showing that these peaks *do* originate from the 1/1 AC as conjectured. On the other hand, the peaks at $2\theta = 31.8^\circ$ and 36.9° were found

to be observed only in the *i* QC sample. Since these reflections can be indexed with the 6D indices of primitive icosahedral lattice, such as 111000 and 111100 reflections, and their transition temperature (16.1(3) K) is exactly the same as that ($T_C = 16$ K) obtained from the bulk measurements, we have come to conclusion that the latter magnetic peaks are due to the *i* $\text{Au}_{65}\text{Ga}_{20}\text{Tb}_{15}$ and a long-range ferromagnetic order is established in *i* $\text{Au}_{65}\text{Ga}_{20}\text{Tb}_{15}$. The details of bulk magnetic properties and magnetic structure of the antiferromagnetic 1/1 AC phase will be reported elsewhere².

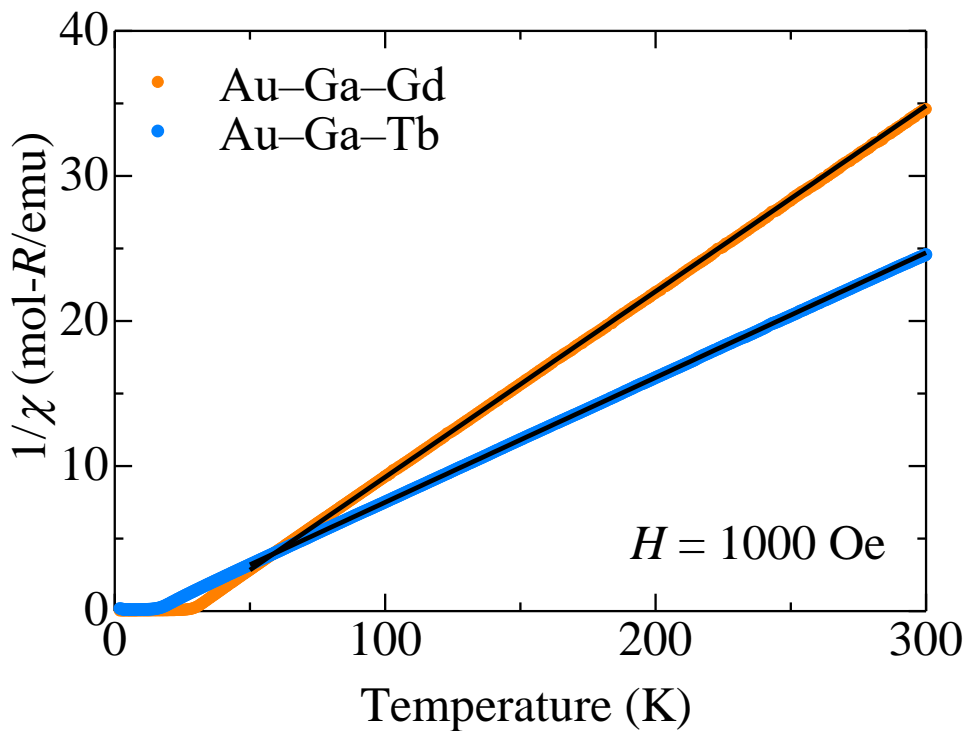


Figure S1 | Temperature dependences of the inverse magnetic susceptibility $1/\chi = H/M$, for the $\text{Au}_{65}\text{Ga}_{20}\text{R}_{15}$ ($\text{R} = \text{Gd}, \text{Tb}$) i QCAs. Magnetic susceptibilities measured under 1000 Oe are shown in the temperature range of 2–300 K. The solid black lines are fits to the Curie-Weiss law between 50–300 K.

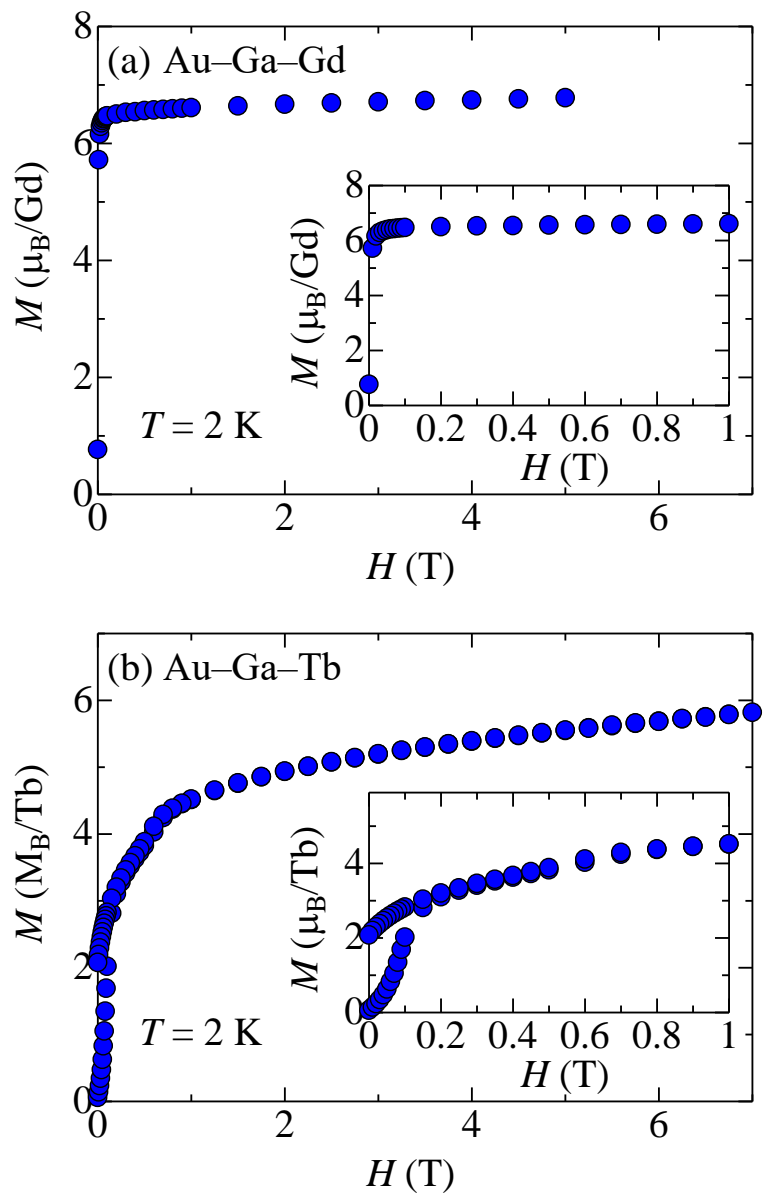


Figure S2 | Magnetic field dependences of the magnetization M , for (a) the $\text{Au}_{65}\text{Ga}_{20}\text{Gd}_{15}$ and (b) $\text{Au}_{65}\text{Ga}_{20}\text{Tb}_{15}$ i QCs. Magnetizations of the $\text{Au}_{65}\text{Ga}_{20}\text{Gd}_{15}$ and $\text{Au}_{65}\text{Ga}_{20}\text{Tb}_{15}$ i QCs measured at 2 K are shown in the magnetic field range of 0 – 7 T. The insets show field dependences of the magnetization in the low field region.

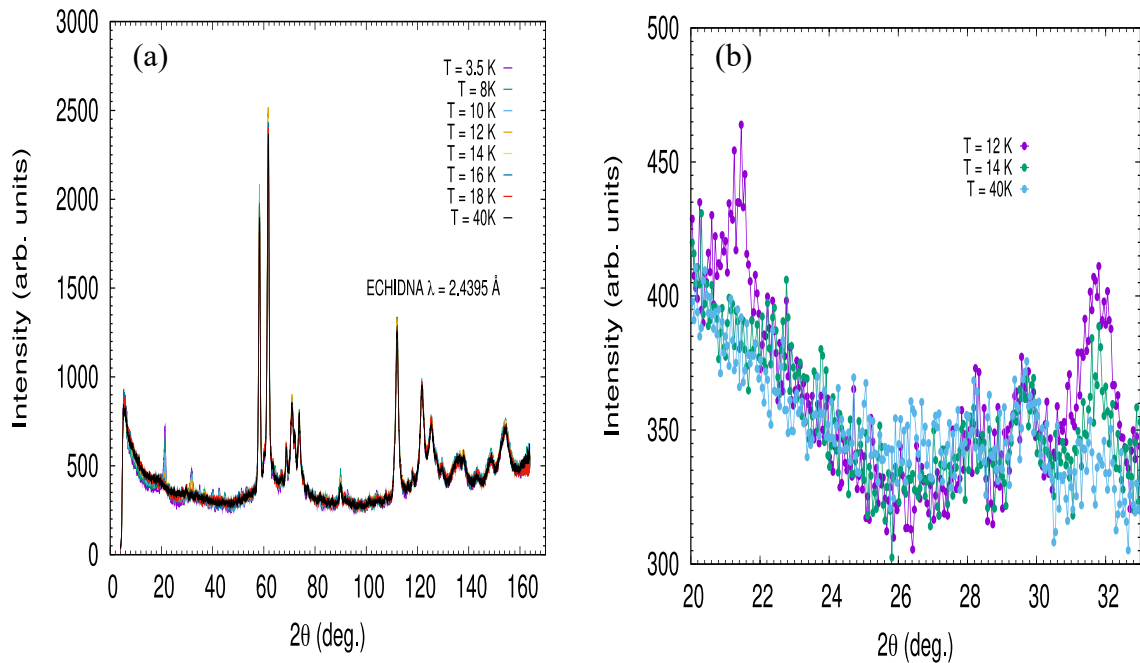


Figure S3 | (a) Neutron-powder-diffraction patterns measured at various temperatures in $3.5 \text{ K} < T < 40 \text{ K}$ for the i Au-Ga-Tb QC sample. (b) Magnified pattern in the low- 2θ region. Data at the selected temperatures across the anomaly temperature of $T_C = 16 \text{ K}$ observed in the bulk magnetic measurements are shown. It can be clearly seen that the peak at 21.4° disappears at $T = 14 \text{ K}$, whereas that at 31.8° retains some intensity, implying that the peak at 21.4° is of a different origin.

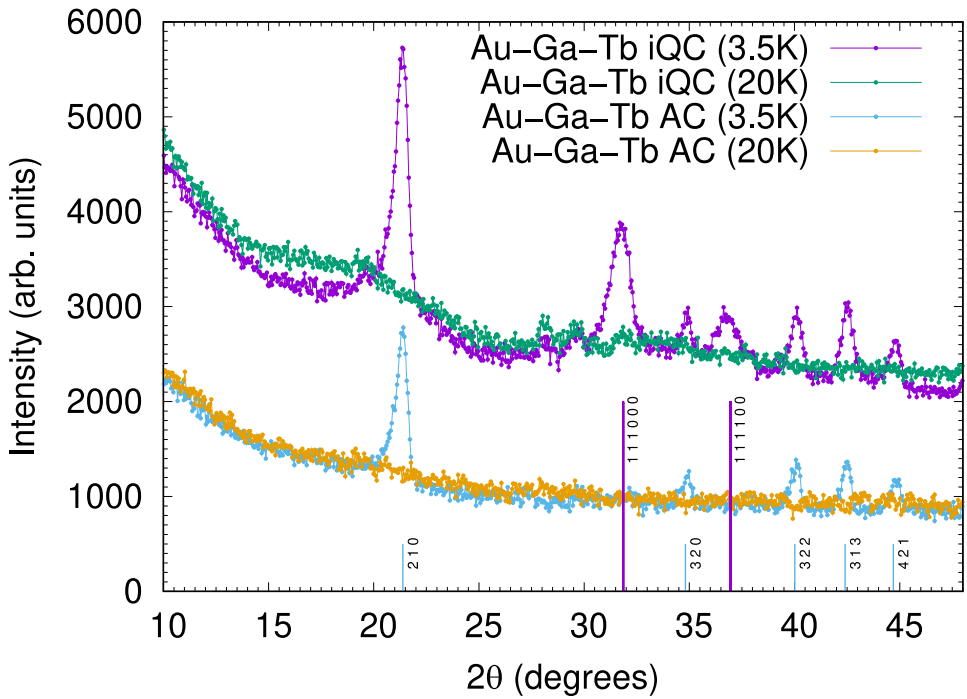


Figure S4 | Neutron-powder-diffraction patterns for the *i* QC and 1/1 AC samples at the base (3.5 K) and paramagnetic (20 K) temperatures. The light-blue and violet vertical lines represent the reflection positions of the antiferromagnetic AC phase and ferromagnetic *i* QC phase, respectively. Note that the peaks at 21.4° , 34.8° , 40.0° , 42.4° and 44.7° coincide with the 210, 320, 322, 313 and 421 magnetic peaks of the 1/1 AC, indicating that they are due to the antiferromagnetic 1/1 AC.

Supplemental References

1. Sato, T. J. *et al.* Whirling spin order in the quasicrystal approximant $\text{Au}_{72}\text{Al}_{14}\text{Tb}_{14}$.
Phys. Rev. B **100**, 054417 (2019).
2. Nawa, K. *et al.* in preparation.